The Statistics of Isoplanatic Angle and Adaptive Optics Time Constant derived from DIMM Data

Venice 2001
Beyond Conventional Adaptive Optics

M. Sarazin[a], A. Tokovinin[b]

[a]European Southern Observatory, D85748 Garching, Germany
[b]Cerro Tololo Inter-American Observatory, Casilla 603, La Serena, Chile

ABSTRACT

The performance of Adaptive Optics and Interferometry depends on several parameters of the atmospheric turbulence: seeing, time constant τ_0, and isoplanatic angle θ_0. It is very challenging to design reliable instruments capable of monitoring them from remote sites. We propose here new simplified methods to extract τ_0 and θ_0 from the data of standard portable seeing monitors (DIMMs). They rely on the analyses and forecasts of synoptic atmospheric parameters produced daily by global meteorological models. Using the results of balloon borne microthermal soundings performed at the VLT and Gemini sites, it is shown that the wind velocity at 12 km above sea level is strongly correlated to the average wavefront velocity, permitting to compute τ_0. Similarly, this velocity can be used to remove the finite-exposure-time bias in the DIMM scintillation data, leading to an estimate of θ_0. The statistics of these parameters at Cerro Paranal is given for the year 2000. Global wind pattern suggests that longer time constants are expected at equatorial and polar sites.

1. INTRODUCTION

Almost all modern large telescopes are now being equipped with Adaptive Optics (AO) systems to compensate turbulence and to push the resolution to the diffraction limit at least at near-infrared wavelengths (Roddier, 1999). Good atmospheric seeing is even more critical to the AO operation than it is for classical seeing-limited observing. Moreover, atmospheric time constant τ_0 and isoplanatic patch size θ_0 are additional parameters which need to be known. Ideally, the vertical turbulence profile should also be monitored to assist AO operation.

Differential Image Motion Monitors (DIMMs) are now widely used for routine seeing measurements in many observatories as well as for site surveys in remote places (Giovanelli et al., 2001). In the DIMM method (Sarazin & Roddier, 1990), the long exposure FWHM of a large telescope limited by the atmosphere is inferred from the variance of the differential tilt of the wavefront measured through twin apertures. Because of signal to noise and hardware limitations, most of these devices have exposure times which are not short enough to freeze the atmospheric tilt motion over their pupils. A posteriori temporal bias correction methods have been proposed, in particular the interlacing of exposures with variable exposure time (Sarazin, 1997), which allows to cancel temporal averaging effects without any information on the speed and direction of the wavefront corrugations.

An extension of the DIMM theory to measurements of the variance of the differential tilt velocity has been proposed by Lopez (1992) in view of estimating the coherence time τ_0 of atmospheric turbulence. However this method requires even shorter exposure times of the order of 1 ms which are only practical with sub-apertures larger than those used in most portable systems. On the basis of vertical profiles of atmospheric turbulence and wind velocity obtained during the balloon launching campaigns at Cerro Paranal in 1993 (Fuchs & Vernin, 1996) and at Cerro Pachon in 1998 (Vernin et al., 2000), we show that there exists -in Northern Chile at least- a consistent relationship between the mean horizontal velocity V_0 of the wavefront corrugations integrated along the line of sight and the wind flow at the tropopause. Combined with instantaneous seeing measurements, it is then possible to produce real-time estimates of the coherence time τ_0 using synoptic analyses of atmospheric circulation delivered daily by the medium range forecasting institutes NCAR in the US and ECMWF in Europe.

The isoplanatic angle θ_0 can be estimated from the fluctuations of stellar flux received by the DIMM sub-apertures and caused by scintillations. It has been noted already by Loos & Hogge (1979) that the scintillation

E-mail: msarazin@eso.org, atokovinin@ctio.noao.edu

index in a 10-cm aperture can lead to an approximate estimation of θ_0. Better approximations are possible with special concentric annular apertures (Krause-Polstorf et al., 1993). Again, because of the too long exposure time of current DIMMs, the scintillation index is generally reduced by time averaging. However, this bias can be calculated providing that one has some real-time knowledge of the temporal spectrum of the scintillation. A practical method to eliminate the bias is proposed and verified with the help of several real profiles of turbulence and wind. This method is further supported by the scintillation data from the GSM instrument (Ziad et al., 2000).

2. CORRECTION OF DIMM SEEING FROM TEMPORAL AVERAGING

The temporal averaging of the variance of the differential motion with a finite exposure time T depends both on the average velocity V_0 and on the direction of the displacement of the wavefront corrugations with respect to the DIMM apertures. The exact computation of this effect (Martin et al., 1987) for a typical experimental setup (distance of the apertures equal to twice their diameter d) and typical operating conditions ($1 < V_0 T/d < 5$) shows that the differential tilt variance σ^2 presents in all cases an exponential dependency on the exposure time T of the type:

$$\sigma^2(T) = \sigma^2(0)\exp(-aT), \tag{1}$$

where the coefficient a is of course unknown and depends on atmospheric conditions. However, performing two simultaneous measurements with exposure times T_1 and T_2 such that $T_2 = 2T_1$, the coefficient a can be eliminated and the bias can be removed by computing

$$\sigma^2(0) = \frac{\left[\sigma^2(T_1)\right]^2}{\sigma^2(T_2)}. \tag{2}$$

In practice the two variances are calculated over two interlaced time series (Sarazin, 1997) or, when possible, on a single time series by rebinning the individual exposures (Ziad et al., 2000). The amount of correction is naturally site-dependent but often not to be neglected. It was noted by Giovanelli et al. (2001) that, at the northern Chile high-altitude sites, the median values of the 0 ms seeing vary between $0.65''$ and $0.76''$, those of the 10 ms seeing between $0.56''$ and $0.65''$ while those of the 20 ms seeing between $0.48''$ and $0.56''$.

3. ESTIMATE OF THE COHERENCE TIME

The wavefront coherence time τ_0 relevant for adaptive optics is given by Roddier (1981):

$$\tau_0 = 0.31\frac{r_0}{V_0}, \tag{3}$$

where V_0 is the average velocity of the turbulence defined by Roddier et al. (1982)

$$V_0 = \left[\frac{\int_0^\infty C_n^2(h)V(h)^{\frac{5}{3}}\mathrm{d}h}{\int_0^\infty C_n^2(h)\mathrm{d}h}\right]^{\frac{3}{5}}. \tag{4}$$

The direct calculation of V_0 or τ_0 is thus only possible when the vertical profiles of the turbulence $C_n^2(h)$ and of the wind velocity $V(h)$ are simultaneously available. Using a combination of classical meteorological radiosondes and home-made microthermal sensors, several campaigns have been conducted worldwide by the Department of Astrophysics of Nice University, and in particular at Cerro Paranal (Fuchs & Vernin, 1995), the site of the ESO VLT (24°37'S, 70°24'W), and at Cerro Pachon (Vernin et al., 2000), the site of Gemini, about 800 km to the south.

In spite of a slightly different geographic situation (Paranal is only 10 km away from the Pacific coast while Pachon is more inland and closer to the cordillera), an analysis of the results obtained at the two sites shows a clear relationship between V_0 and the wind velocity at 200 mb (about 12 km above sea level). As shown in Fig. 1, after forcing the best fit of 35 balloon flights to pass through the coordinate origin, one obtains the expression $V_0 \simeq 0.4V_{200mb}$. The relative accuracy of the method improves linearly with V_{200mb} from 30% at 20 m/s to better than 20% above 40 m/s ($V_0 > 16$ m/s). The two flights presenting the largest errors ((X,Y)$\approx$(16,14) on Fig. 1) were launched on the same night at Paranal. This night was the only circumstance when the high altitude wind velocity was much lower than at ground level. In such a case, a better agreement was obtained taking $V_0 = V_{ground}$. A more general formula is thus proposed

$$V_0 \simeq Max(V_{ground}, 0.4V_{200mb}); \quad \mathrm{rms} = 2.6 \text{ m/s} \tag{5}$$

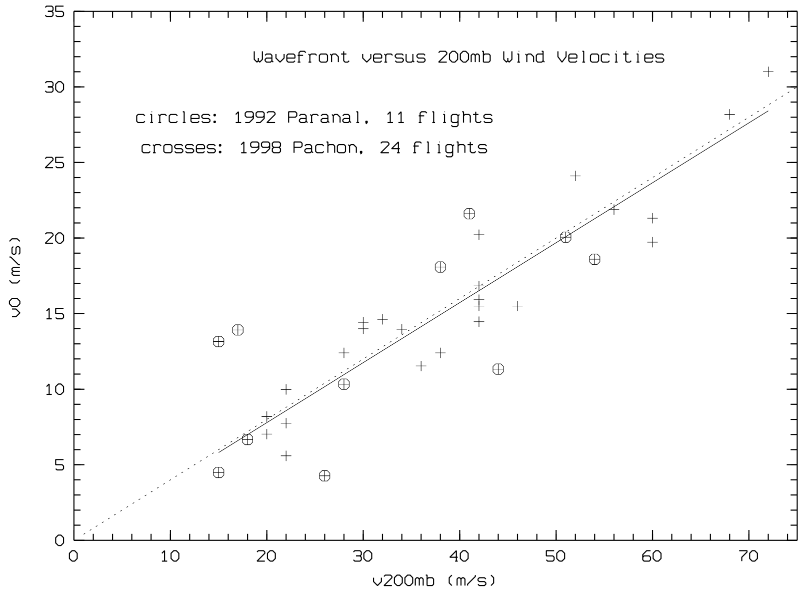

Figure 1. Proportionality between the wind velocity at 200 mb V_{200mb} and the wavefront velocity V_0 measured over 35 balloon flights at Paranal (crossed circles) and at Pachon (crosses). The full line corresponds to the best least squares fit, the dotted line corresponds to $V_0 = 0.4V_{200mb}$.

which leads to an estimate of τ_0 within relative mean and rms errors of 4% and 19% respectively over the 35 balloon flights. As could be expected, this method produces a larger error when the bulk of the turbulence is close to the ground. More precisely, in two flights showing an error larger than 50% , the turbulence characteristic altitude $\bar{H} = 0.314\, r_0/\theta_0$ (Fried, 1976) is smaller than 3 km while the average of the 35 flights is 6.4 km.

Following the pioneering work of Vernin (1986), these considerations have immediate consequences for selecting the sites of the next generation of telescopes: with moderate wind at ground level and at equal seeing quality, the existing and potential astronomical sites can be ranked in terms of suitability for adaptive optics simply by looking at the global circulation of the wind at 200 mb. Figs. 2 and 3 were built from the 2.5 degree resolution NOAA Global Gridded Upper Air database using the 16-year (1980-1995) statistics of climatic summaries produced by the model of the European Center for Medium Range Weather Forecasts (ECMWF). They show the superiority of polar and equatorial areas over mid-latitude sites. Seasonal effects must also be taken into account in any site analysis as shown in Table 1 where the observatories of Paranal and La Silla appear similar to Mauna Kea in December but have wind almost twice faster in June. When a higher horizontal resolution is required, a direct mapping of τ_0 has been proposed by Masciadri & Garfias (2001) using a meso-scale non-hydrostatic model to simulate turbulence and wind profiles in a region of some kilometers around a site.

Table 1. Comparison of the mean 200 mb wind velocity in m/s at Mauna Kea, Paranal and La Silla

Month	Mauna Kea	Paranal	La Silla
December	24.7	22.2	27.6
June	19.5	34.5	36.0

4. ESTIMATE OF THE ISOPLANATIC ANGLE

Scintillation index s is defined as a variance of the natural logarithm of the light intensity received by an aperture of the instrument. A theory of light propagation through atmosphere (Roddier, 1981) in the limit of faint perturbations relates the index to the vertical profile of the refractive index structure constant $C_n^2(h)$:

$$s = \int_0^{Z_{max}} \mathrm{d}z\; C_n^2(z) W(z), \tag{6}$$

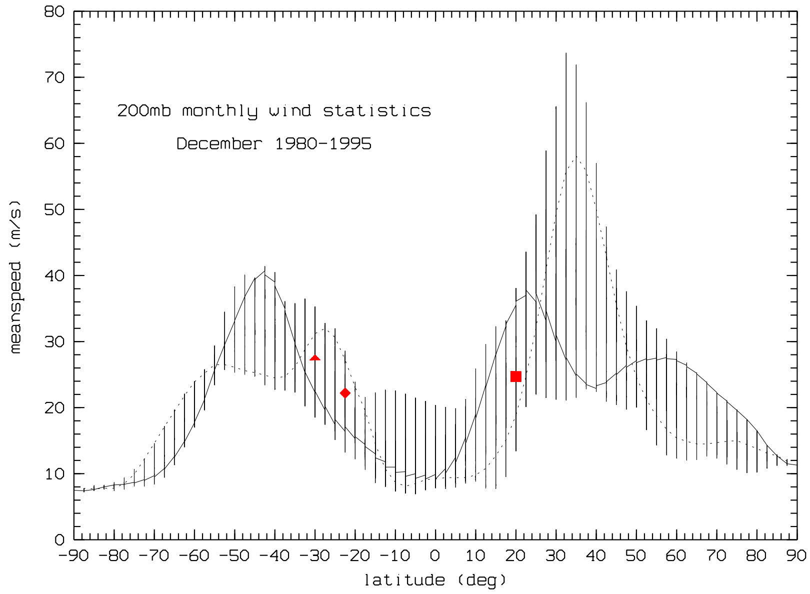

Figure 2. 200 mb mean wind velocity during the month of December from 1980 to 1995 as a function of latitude for all longitudes (vertical bars) and for 0° (full line) and 180° (dashed line) longitudes. The observatories of Mauna Kea, Paranal and La Silla are indicated, respectively, by a filled square, diamond, and triangle.

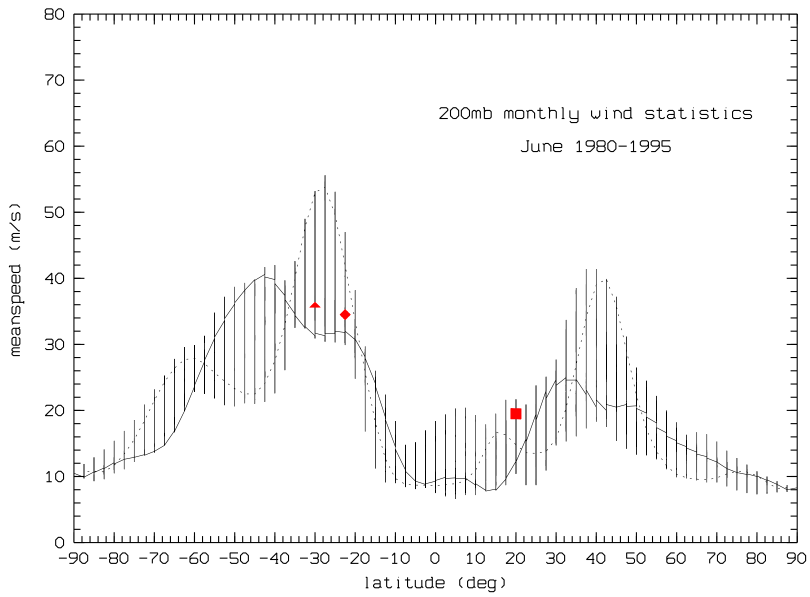

Figure 3. 200mb mean wind velocity during the month of June from 1980 to 1995 as a function of latitude for all longitudes (vertical bars) and for 0° (full line) and 180° (dashed line) longitudes. The observatories of Mauna Kea, Paranal and La Silla are indicated, respectively, by a filled square, diamond, and triangle.

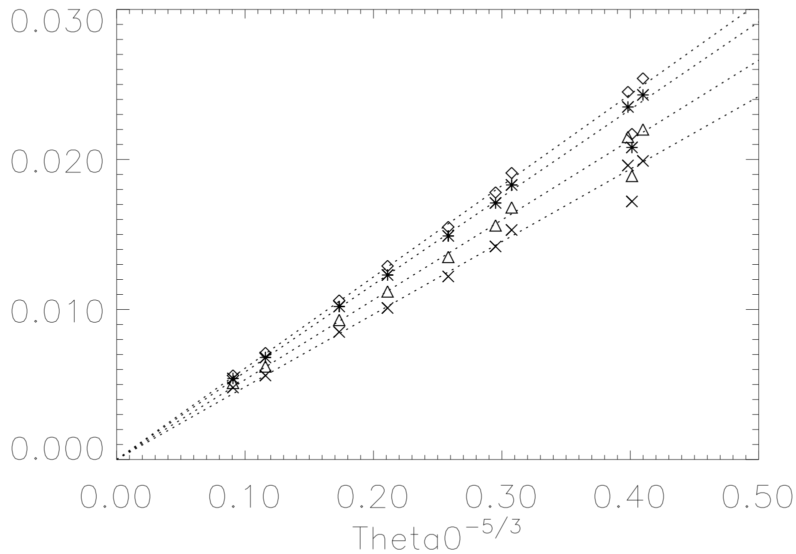

Figure 4. Proportionality between the $\theta_0^{-5/3}$ (in arc-seconds) and the scintillation indices s at the wavelengths of 0.4 μm (diamonds), 0.5 μm (asterisks), 0.7 μm (triangles) and 0.9 μm (crosses). The dotted lines correspond to the average proportionality coefficients.

where the integration over range $z = h \cos\gamma$ is performed from the aperture ($z = 0$) to the maximum distance of turbulence, Z_{max}. The weighting function $W(z)$ depends on turbulence spectrum, wavelength λ, and aperture shape. For finite exposure time τ, $W(z)$ is modified, because the "effective" aperture is extended in the wind direction by $V(h)\tau$, where $V(h)$ is the horizontal wind velocity at the altitude h above the site. Thus, a finite exposure time introduces the bias $R(\tau) = s(\tau)/s(0)$ in the measured scintillation index, which can be computed from the vertical profiles $C_n^2(h)$ and $V(h)$ (Tokovinin, 2001).

The isoplanatic angle for adaptive optics θ_0 at zenith is defined as (Fried, 1982)

$$\theta_0^{-5/3} = 2.91(2\pi/\lambda)^2 \int_0^{H_{max}} \mathrm{d}h \; h^{5/3} C_n^2(h). \tag{7}$$

Loos & Hogge (1979) noted the similarity of this expression with (6), and suggested that θ_0 can be derived from scintillation index if the weighting function is roughly proportional to $h^{5/3}$. For an aperture of about 10 cm in diameter and for $\lambda = 0.5\mu$m the approximation $W(z) \propto z^{5/3}$ holds well at altitudes around 10 km, which mostly contribute to scintillation. We calculate the isoplanatic angle (at zenith and at 0.5μm) from the scintillation index s measured at zenith angle γ by the formula (Ziad et al., 2000)

$$\theta_0 = A s^{-3/5} (\cos\gamma)^{-8/5}. \tag{8}$$

It is not clear, however, which value of the ratio $W(z)/z^{5/3}$ should be selected to compute the calibration constant A, and how this constant depends on λ. To elucidate the problem, we took 11 real turbulence profiles measured in 1992 at Cerro Paranal (Fuchs & Vernin, 1995). Scintillation indices and θ_0 at zenith were calculated for each profile. The proportionality between s and $\theta_0^{-5/3}$ implied by Eq. (8) is tested in Fig. 4 for the 4 different wavelengths. As can be seen, the deviation from proportionality is actually quite small, ranging from 4.4 % to 5.1 % rms for wavelengths from 0.4 to 0.9 μm. Taking the average ratio between s and $\theta_0^{-5/3}$ and transforming it into A, we get $A = 0.186, 0.182, 0.172, 0.162''$ for $\lambda = 0.4, 0.5, 0.7, 0.9$ μm, respectively. With these numbers we estimate the error on θ_0 that may arise from the imprecise knowledge of the mean wavelength in a DIMM observing stars of different spectral type without filter. Supposing that the calibration coefficient for λ =0.5 μm is used, and that the actual wavelength may change from 0.4 to 0.7 μm, the errors would be +2 % and -5 %, respectively.

The exposure time bias $R = s(\tau)/s(0)$ must be taken into account in the computation of θ_0: for a single layer traveling with speed $V > 35$ m/s at 10 km altitude, R drops below 0.5 for an exposure time $\tau = 5$ ms.

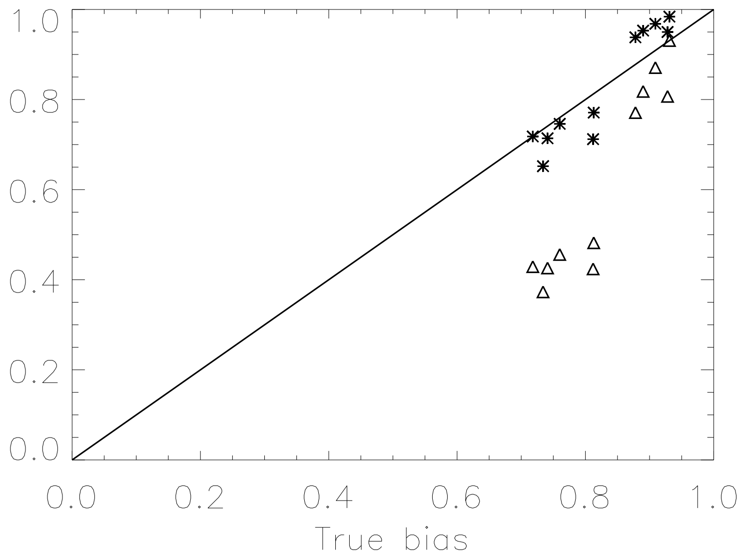

Figure 5. The scintillation exposure time bias for a single-layer model $R_{0.5V_{200mb}}$ (asterisks) is plotted against the true bias $R_{V(h)}$ for the 11 profiles at Cerro Paranal. The full-velocity bias $R_{V_{200mb}}$ is shown by triangles.

Our first idea was to use the wind velocities V_{200mb} to correct for this bias, assuming that the whole turbulence can indeed be represented by a single layer. The true bias $R_{V(h)}$ for $\tau = 5$ ms was computed for the 11 balloon profiles at Cerro Paranal from the PARSCA campaign (Fuchs & Vernin, 1995). As can be seen in Fig. 5 (triangles), the true bias is always smaller than the single-layer full velocity bias $R_{V_{200mb}}$.

It has been demonstrated by Coulman et al. (1995) that layers with strong optical turbulence are typically generated at the interfaces between the fast- and slow-moving atmospheric strata. This is indeed the case for the Paranal profiles considered here. When we compute the bias for a single-layer model with the *one half* of the jet stream velocity, the results are very close to the rigorous bias computed from the profiles (Fig. 5, asterisks). For the 11 profiles studied here, the rms difference of "half-speed" and true bias is only 7% and the mean ratio $R_{V(h)}/R_{0.5\,V_{200mb}}$ is 0.995. Thus, we have at hand a practical method to correct the 5 ms scintillation data from DIMM for the finite-exposure bias. Moreover, this correction is not dramatic: for all 11 profiles, $R(5\text{ ms}) > 0.7$.

Another site characterization campaign at Cerro Paranal has been organized in 1998 with the GSM instrument (Martin et al., 2000). Although the main purpose of this campaign was to measure the wavefront outer scale, scintillation indices were also obtained as a by-product. The exposure time of GSM is 5 ms. By binning data, a 10 ms exposure was obtained, and the scintillation index was linearly extrapolated to zero exposure time (Ziad et al., 2000). We compared the nightly average ratio of 10 ms and 5 ms indices to the same ratio computed for a single layer at 10 km with a velocity of the jet stream, V_{200mb} and half of V_{200mb} successively. A much better agreement was found with the later, thus confirming our idea to correct the exposure bias using half of the jet stream speed.

5. RESULTS AT PARANAL FOR THE YEAR 2000

Based on the methodology developed in the previous sections, seeing, coherence time and isoplanatic angle are routinely monitored by a DIMM at Paranal. We present here the statistics for the full year 2000, based on about 170000 samples of seeing and scintillation. The data is filtered with a 10 mn wide gaussian window. The wind at 200 mb is linearly interpolated from the 6-hourly ECMWF 00 UT forecasts. As the scintillation cannot be measured when the atmospheric absorption is variable, the statistics given in Figs. 6 and 7 and summarized in Table 2 refer to samples taken during photometric sky only. A photometric sky is defined by a line of sight variability of the stellar flux smaller that 1.5% rms over the time averaging window.

There is no systematic relation between either seeing or isoplanatic angle and the wind at 200 mb, but one notices slow trends in the mean values. Because high altitude turbulence generally represents a small fraction of the total, the mean seeing is fairly independent of the 200 mb wind, and starts increasing by about 10% per 10 m/s above 40 m/s only. Thus the tropopause wind is not a robust criterion for selecting sites with good seeing. Similarly and in spite of the $h^{5/3}$ weighting, the mean isoplanatic angle increases slowly, although regularly, with decreasing 200 mb wind speed at a rate of about 10% per 10 m/s with an average of 2.0″ above 40 m/s, 2.7″ between 40 m/s and 20 m/s, and 3.2″ below 20 m/s . This weak dependency means that, on an average, the jet does not increase significantly the level of turbulence at high altitude but rather makes it move faster. In this respect, the seasonal variations of upper atmospheric circulation clearly affect the coherence time at Paranal which decreases from a median (50 percentile) value of 4.9 ms in the most favorable period (January-March) to 2.5 ms in May-July.

Table 2. Summary of AO related observing conditions at Paranal during 2000, for observation at 0.5 μm, at zenith, averaged over 10 mn. Data is not corrected for a finite outer scale of the turbulence.

Parameter	best 5%	best 20%	50%	mean
Seeing, arcsec	0.43	0.56	0.75	0.86
200mb Wind, m/s	12	19	29	32
τ_0, ms	8.5	5.8	3.6	3.9
θ_0, arcsec	4.1	3.3	2.6	2.6

REFERENCES

Coulman C.E., Vernin J., Fuchs A., *Optical seeing – mechanism of formation of thin turbulent laminae in the atmosphere*, Appl. Opt., **34**, pp. 5461-5474, 1995.

Fried D.L., *Imaging through the atmosphere*, SPIE Proc, **75**, 20, 1976.

Fried D.L., *Anisoplanatism in adaptive optics*, J. Opt. Soc. Amer. A., **72**, pp. 52-61, 1982.

Fuchs A., Vernin J. , Final Report on PARSCA 1992 and 1993 campaigns, ESO Report VLT-TRE-UNI-17400-0001, 1996.

Giovanelli R., Darling J., Sarazin M., Yu J., Harvey P., Henderson C., Hoffman W., Keller L., Barry D., Cordes J., Eikenberry S., Gull G., Harrington J., Smith J.D., Stacey G., Swain M., *The Optical/Infrared Astronomical Quality of High Atacama Sites. I. Preliminary Results of Optical Seeing*, PASP 2001 (sub).

Krause-Polstorf J., Murphy E.A., Walters D.L., *Instrumental comparison: corrected stellar scintillometer versus isoplanometer*, Appl. Opt., **32**, pp. 4051-4057, 1993.

Loos G., Hogge C., *Turbulence of the upper atmosphere and isoplanatism,* Appl. Opt., **18**, pp. 2654-2661, 1979.

Lopez B., *How to monitor exposure times for high resolution imaging modes*, Astron. Astrophys., **253**, pp. 635-640, 1992.

Martin F., Conan R., Tokovinin A., Ziad A., Trinquet H., Borgnino J., Agabi A., Sarazin M., *Optical parameters relevant for High Angular Resolution at Paranal from GSM instrument and surface layer contribution*, Astron. Astrophys. Suppl. Ser., **144**, pp. 39-44, 2000.

Martin H.M., *Image Motion as a Measure of Seeing Quality*, PASP, **99**, 1360, 1987.

Masciadri E., Garfias T., *Wavefront coherence time seasonal variability and forecasting at the San Pedro Martir site*, Astron. Astrophys., **366**, pp. 708-716, 2001.

Roddier F., *The effects of atmospheric turbulence in optical astronomy*, in Progress in Optics, E. Wolf ed., Vol. XIX, pp. 281-376, 1981.

Roddier F., Gilli J.M., Lund G., *On the origin of speckle boiling and its effect in stellar speckle interferometry*, J. of Optics, **13**, 5, 1982.

Roddier F., ed., *Adaptive optics in astronomy*, Cambridge Univ. Press: Cambridge, 1999.

Sarazin M., Roddier F., *The E.S.O Differential Image Motion Monitor*; Astron. Astrophys., **227**, pp. 294-300, 1990.

Sarazin M., *Automated Seeing Monitoring for Queue Scheduled Astronomical Observations*, Proc. SPIE, **3125**, pp. 366-374, 1997.

Tokovinin A., *Measuring seeing and atmospheric time constant by differential scintillations*, Appl. Opt., 2001 (sub).

Vernin J., *Astronomical site selection: a new meteorological approach*, Proc. SPIE, **628**, pp. 142-147, 1986.

Vernin J., Agabi A., Avila R., Azouit M., Conan R., Martin F., Masciadri E., Sanchez L., Ziad A., *1998 Gemini site testing campaign. Cerro Pachon and Cerro Tololo*, Gemini RPT-AO-G0094, 2000.

Ziad A., Conan R., Tokovinin A., Martin F., Borgnino J., *From the Grating Scale Monitor (GSM) to the Generalized Seeing Monitor (GSM)*. Appl. Opt., **39**, pp. 5415-5425, 2000.

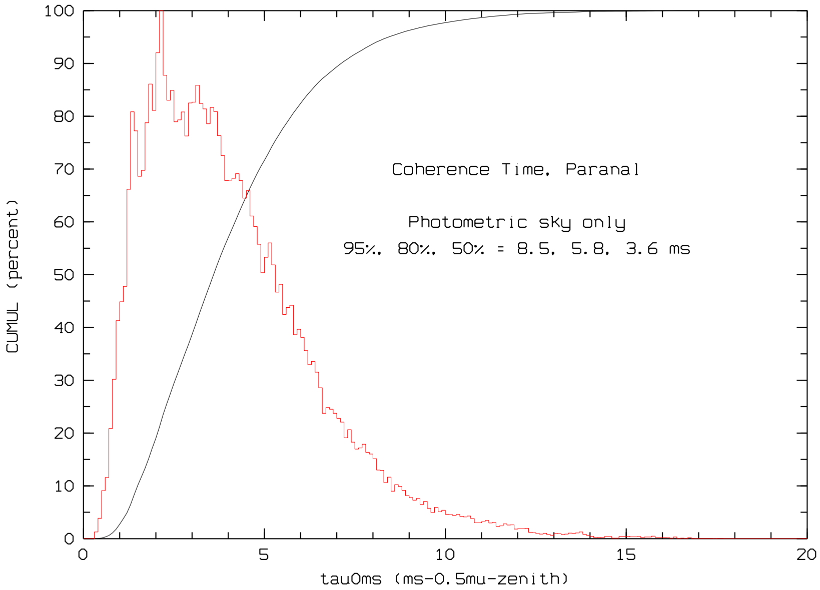

Figure 6. Statistics of the coherence time τ_0 at Cerro Paranal for the year 2000 (ms at 0.5 μm at zenith).

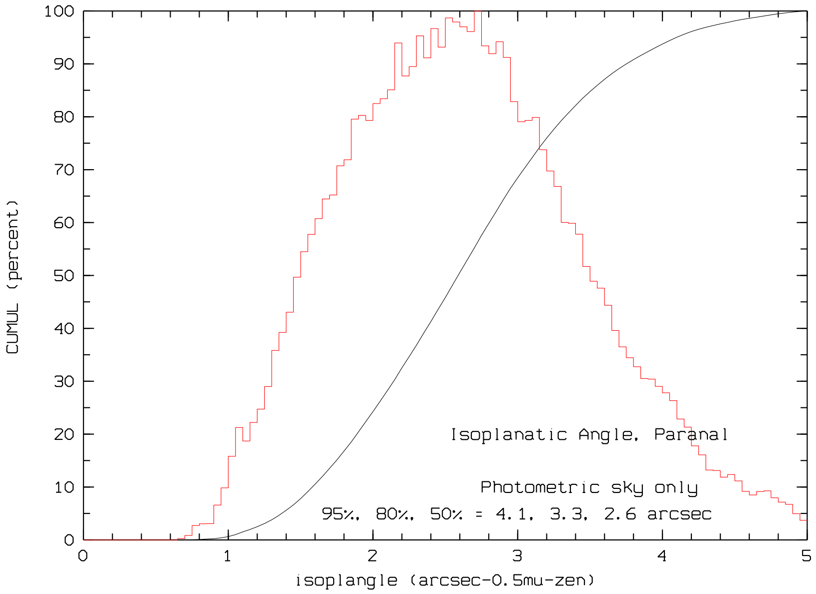

Figure 7. Statistics of the isoplanatic angle θ_0 at Cerro Paranal for the year 2000 (arcseconds at 0.5 μm at zenith).